Scripta Materialia 153 (2018) 104–108

Contents lists available at ScienceDirect

Scripta Materialia

journal homepage: www.elsevier.com/locate/scriptamat

Regular article

# Nitrogen doped cuprous oxide as low cost hole-transporting material for perovskite solar cells

Guifang Han [a,1], Wen Han Du [b,c,1], Bao-Li An [d], Annalisa Bruno [a], Shin Woei Leow [c], Cesare Soci [e], Sam Zhang [f], Subodh G. Mhaisalkar [a,c], Nripan Mathews [a,c,*]

[a] Energy Research Institute @NTU (ERI@N), Nanyang Technological University, Research Techno Plaza, X-Frontier Block, Level 5, 50 Nanyang Drive, 637553, Singapore
[b] Changzhou Institute of Technology, Changzhou, Jiangsu, 213002, P.R. China
[c] School of Materials Science and Engineering, Nanyang Technological University, Nanyang Avenue, 639798, Singapore
[d] Department of Chemistry, College of Science, Shanghai University, Shanghai, 200444, P.R. China
[e] Division of Physics and Applied Physics, School of Physical and Mathematical Sciences, Nanyang Technological University, 21 Nanyang Link, 637371, Singapore
[f] Faculty of Materials and Energy, Southwest University, Chongqing, 400715, P.R. China

ARTICLE INFO

*Article history:*
Received 26 March 2018
Received in revised form 27 April 2018
Accepted 28 April 2018
Available online xxxx

*Keywords:*
Perovskite
Solar cell
Hole-transporting material
Nitrogen doped cuprous oxide

ABSTRACT

Substituting expensive traditional hole transporting material (HTM) with cheaper inorganics is a key factor for perovskite photovoltaics commercialization. $Cu_2O$ is a promising *p*-type semiconductor exhibiting good band-alignment with perovskite. However, due to solvent and temperature incompatibility, $Cu_2O$ is typically employed in inverted configuration, where an even more expensive, unstable Phenyl-C61-butyric acid methyl ester is necessary as an electron-transporting layer. Therefore, we explored the use of sputtered nitrogen-doped $Cu_2O$ directly on halide-perovskite as a HTM. With a thin interfacial layer, efficiency of 15.73% was achieved. This work indicates the possibility of low cost sputtered inorganics as HTM for efficient perovskite photovoltaics.



Organic-inorganic halide perovskite solar cell has opened a new era for high efficiency solution processed thin film photovoltaics [1–5]. Efforts in composition design [6,7], process modification [8], investigation of dominant recombination mechanism [9,10] and therefore strategies to improve the performance of perovskite solar cells [11], have led to a record power conversion efficiency more than 22%. A typical perovskite solar cell architecture consists of electron transporting layer, perovskite absorber and hole transporting material layered either in a conventional or an inverted configuration [1,12]. The perovskite absorber layer as well as the hole-transporting layer, (typically Spiro-MeOTAD), can be solution processed by simple spin coating. However, the high cost of Spiro-MeOTAD poses a major obstacle in the path of large-scale commercialization of perovskite solar cells [13]. Inorganic *p*-type semiconductors, especially Cu-based materials such as copper iodide (CuI), copper thiocyanate (CuSCN), and cuprous oxide ($Cu_2O$) [14–16], has recently attracted significant attention as hole-transporting materials (HTM) owing to their high mobility and low fabrication cost. CuI is the first reported inorganic Cu-based HTM for perovskite solar cell but achieved a low efficiency of ~6%. CuSCN has been reported recently as HTM to obtain a power conversion efficiency of more than 20% with a better stability [15]. However, not many solvents are available that could readily dissolve CuSCN. Diethyl sulfide which is presently utilized, is not environmentally benign and also has an affinity to dissolve perovskite requiring careful processing. $Cu_2O$ has been investigated for many years due to its unique *p*-type semiconducting properties. Appropriate energy band alignment along with its low cost and environmental friendliness makes $Cu_2O$ an excellent candidate as HTM for perovskite solar cells. $Cu_2O$ has been reported successfully as an HTM for perovskite in inverted structure with phenyl-C61-butyric acid methyl ester (PCBM) as electron transporting layer on top [17–20]. The $Cu_2O$ is firstly deposited on Indium tin oxide substrate using solution process such as successive ionic layer absorption and reaction, or spin coating using $Cu(acac)_2$ as the precursor [17,18]. Subsequently, the perovskite is spun coated on the $Cu_2O$ layer, followed by a PCBM electron transport layer. This inverted (*p-i-n*) configuration is utilized due to the tendency of the $Cu_2O$ deposition processes to degrade the perovskite layer below it due to the solvents or the temperatures applied. PCBM, in addition to being less cost-effective than Spiro-MeOTAD, is also not stable at ambient atmosphere. Another limitation is the optical absorption that could happen in the $Cu_2O$ when applied in the inverted configuration. $Cu_2O$ with a bandgap of around 2.21 eV [20], will absorb light with wavelength less than 560 nm, which will

* Corresponding author at: Energy Research Institute @NTU (ERI@N), Nanyang Technological University, Research Techno Plaza, X-Frontier Block, Level 5, 50 Nanyang Drive, 637553, Singapore.
*E-mail address:* Nripan@ntu.edu.sg (N. Mathews).
[1] These authors contribute equally to this work.

https://doi.org/10.1016/j.scriptamat.2018.04.049
1359-6462/

decrease the light absorption in perovskite. All these factors dramatically weaken the advantage of using $Cu_2O$ as HTM for perovskite solar cells in an inverted configuration. Therefore, the best way to use $Cu_2O$ is to directly or partially substitute the Spiro-MeOTAD layer in a conventional perovskite solar cell configuration. Magnetron sputtering is a promising technique to fabricate uniform, dense and pin-hole free films without considering the issues of solvent compatibility [21]. However the heat generated and the kinetic energy of the atoms in the sputtering may affect the perovskite layer and hence the performance of devices. Ahmadi et al. carefully adjusted the tilting angle of substrate against the sputtering target and obtained a uniform and compact $Cu_2O$ film on top of perovskite layer with a device efficiency of 8.93% [22]. Since most commonly used HTMs, including inorganics and organics, have relatively poor conductivity, doping has been proved to be an effective approach to improve their carrier densities. Y. Zhou et al. [23] thoroughly reviewed how doping and alloying improve the electronic properties of electron and hole transporting materials and further the perovskite solar cell performance. Nitrogen (N) has been reported as an effective *p*-type dopant for $Cu_2O$. It is generally believed that N substitute on the oxygen sites ($N_O$). Recently theoretical calculation found that $N_O$ is a deep acceptor and it is unlikely to be the cause of observed increasing of hole concentration [24,25]. Careful defect physics calculation suggested that $N_2$ molecule on Cu's site $(N_2)_{Cu}$ is a shallow acceptor with a low formation energy, which might give hole carriers [24]. This is further confirmed experimentally by electron energy loss spectroscopy revealing that nitrogen is in molecular $N_2$ form in $Cu_2O$ [26]. In this work, we have lowered the sputtering power to avoid damage of perovskite layer and introduced nitrogen doping to further explore $Cu_2O$ as

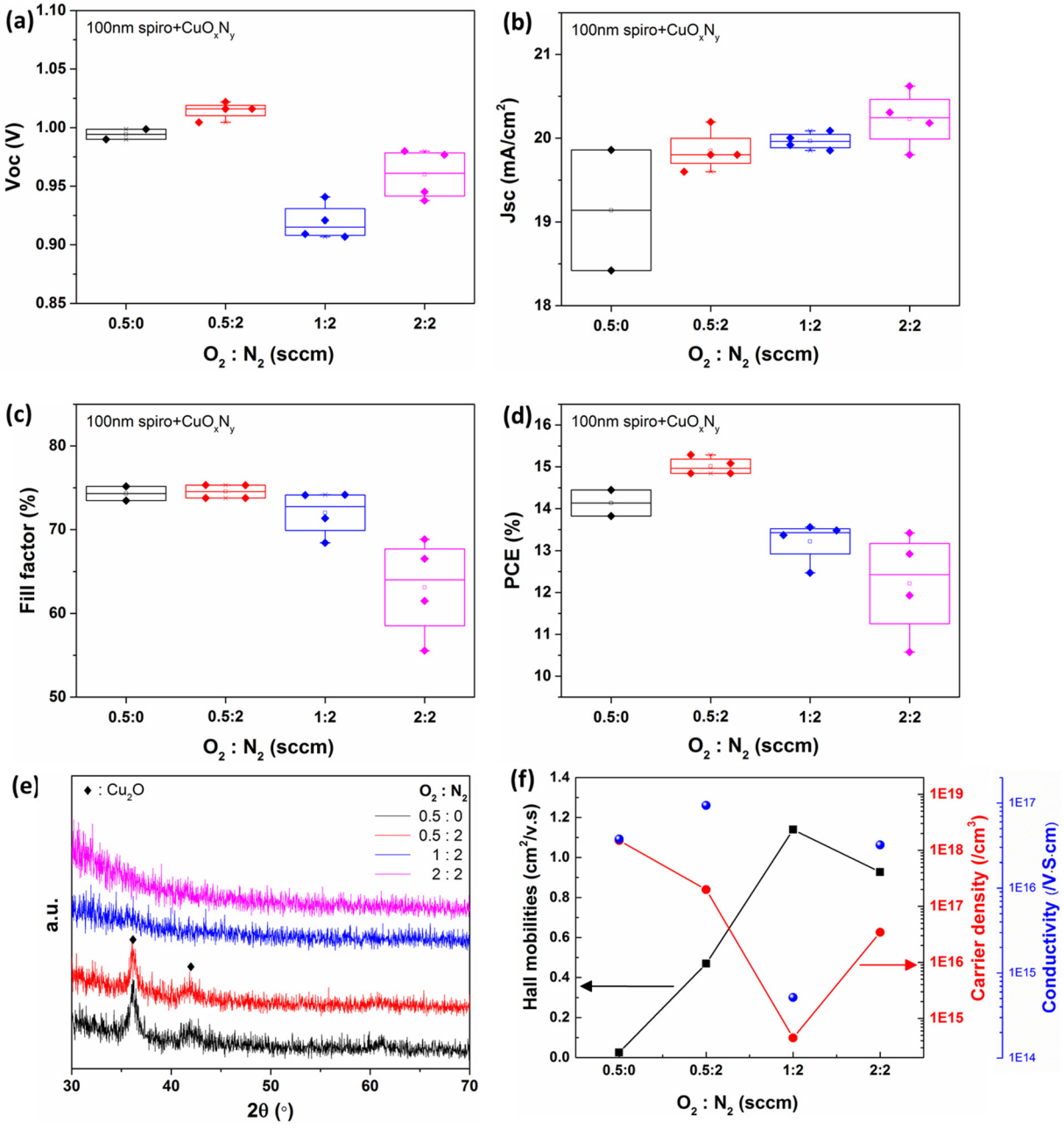


**Fig. 1.** Device performance distribution of characteristic photovoltaic parameters obtained from perovskite based solar cell with $CuO_xN_y$ as hole transporting materials deposited at different $O_2$:$N_2$ ratio: (a) open-circuit voltage ($V_{oc}$), (b) short-circuit current density ($J_{sc}$), (c) fill factor (*FF*) and (d) power conversion efficiency (PCE) at similar device fabrication conditions. 100 nm-thick Spiro-MeOTAD was used as interfacial and protection layer during $CuO_xN_y$ sputtering. (e) XRD spectrums and (f) Hall mobility, carrier density and conductivity of sputtered $CuO_xN_y$ films with different $O_2$:$N_2$ flow ratio.

HTM for enhanced solar cell performance resulting in an efficiency of 15.73%.

To avoid strong damage of perovskite films during the sputtering, a low sputtering power of 15 W (the lowest power attainable in the deposition system) is used for the deposition of all $CuO_xN_y$ films. Performance of devices fabricated with low power sputtered $CuO_xN_y$ (~180 nm) on the halide perovskite layer is presented in Fig. S1. The open-circuit voltage ($V_{oc}$) is around 0.8 V; short-circuit current ($J_{sc}$) is less than 5 mA/cm$^2$ and power conversion efficiency (PCE) is lower than 2%. The current-voltage (*I-V*) curve of best cell is given in Fig. S1 (b) with a PCE of 1.54%. Although low power is applied during sputtering, it is still not able to form a good interface between perovskite and $CuO_xN_y$. There is no noticeable physical damage observable in the cross section microstructure, as can be seen from Fig. S2, indicating that the defects are electronic in nature. To manage the interface, a thin layer of Spiro-MeOTAD is introduced between perovskite and $CuO_xN_y$ as a buffer layer. The device performance shown in Fig. S3 shows a dramatic improvement. The influence of gas composition on the properties of the solar cell was then studied. We fixed the flow rate of oxygen ($O_2$) and varied the flow rate of nitrogen ($N_2$). With increasing $N_2$ flow rate, there is a reduction in the $V_{oc}$, $J_{sc}$ and fill factor (*FF*). The highest efficiency of 13.42% is achieved with an $O_2$:$N_2$ flow rate of 2:2, the lowest $N_2$ flow rate. Then the $N_2$ flow rate was set at 2 sccm and the $O_2$ flow rate varied between 0.5, 1 to 2 sccm. Further decrease of the $O_2$ flow rate resulted in the appearance of zero valence copper. When decreasing the flow rate of $O_2$, increase in $V_{oc}$ and *FF* is observed with a slight decrement of $J_{sc}$. The highest overall efficiency (15.73%) is achieved with a lower $O_2$ flow rate of 0.5 sccm, as shown in Fig. 1. The higher $V_{oc}$ obtained with less $O_2$, might be due to a more favorable band alignment with the small change in stoichiometry of $CuO_xN_y$ films. When comparing the effect of N-doping at same $O_2$ flow of 0.5 sccm, although the *FF* didn't change so much, the overall efficiency is reduced by more than 1% against N-doped cuprous oxide as the HTM primarily due to lower $J_{sc}$ and $V_{oc}$.

The X-ray diffraction patterns of $CuO_xN_y$ sputtered with different $O_2$:$N_2$ ratio are illustrated in Fig. 1(e). It clearly indicated that with low $O_2$ flow rate as 0.5 sccm, $Cu_2O$ phase is formed. However, further increasing the $O_2$ flow rate, the $CuO_xN_y$ films tunes to be amorphous. Interestingly, better device performance is obtained with low $O_2$ flow rate. This might due to the better crystallinity of the $CuO_xN_y$ films. To further figure out the correlation of device performance with the properties of $CuO_xN_y$ films, mobility and carrier density were investigated from Hall measurement are shown in Fig. 1(f). The Hall mobility (black line) increased with the addition of nitrogen reaching a maximum at $O_2$:$N_2$ ratio of 1:2. However, the carrier density (red line) exhibits the opposite trend. Based on these factors, the film conductivity was calculated and plotted in blue (Fig. 1(f)). The highest conductivity is obtained with an $O_2$:$N_2$ ratio of 0.5:2, which is consistent with higher crystallinity of $CuO_xN_y$ films and the corresponding devices performance. The microstructure of sputtered $CuO_xN_y$ films were given in Fig. S4. However, no noticeable difference is observed with different $O_2$:$N_2$ ratio. Therefore, the crystallinity and electronic properties of $CuO_xN_y$ films are more critical for device performance.

With the $O_2$:$N_2$ ratio fixed at 0.5:2, we examine the effect of $CuO_xN_y$ thickness on the performance of the perovskite solar cells. From Fig. 2 (a), the PCE of the perovskite cells peaks at 80 nm $CuO_xN_y$ thickness and decreases subsequently. Based on this optimized condition, 20 devices were fabricated to verify the reproducibility of this process as

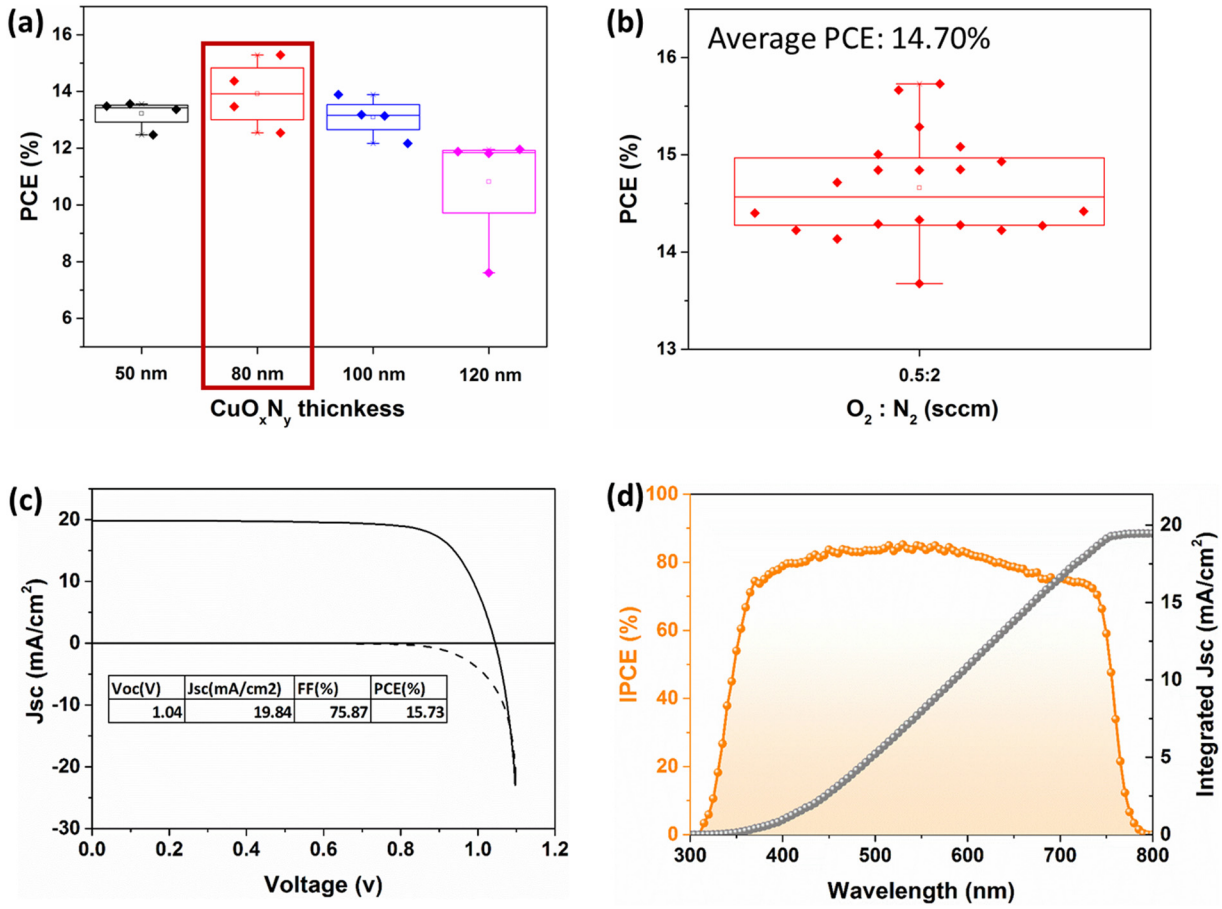


**Fig. 2.** (a) Power conversion efficiency (PCE) of devices with different thickness of $CuO_xN_y$, in which the 80 nm devices give the highest PCE; (b) PCE distribution of perovskite solar cells with Spiro-MeOTAD /$CuO_xN_y$ as hole transporting materials fabricated at optimal condition; (c) Characteristic current density ($J_{sc}$) vs voltage (V) curves of the champion cell fabricated using Spiro-MeOTAD/$CuO_xN_y$ as hole transporting materials; (d) Incident photon-to-current efficiency (IPCE) of best performing device with integrated current density of 19.45 mA/cm$^2$.

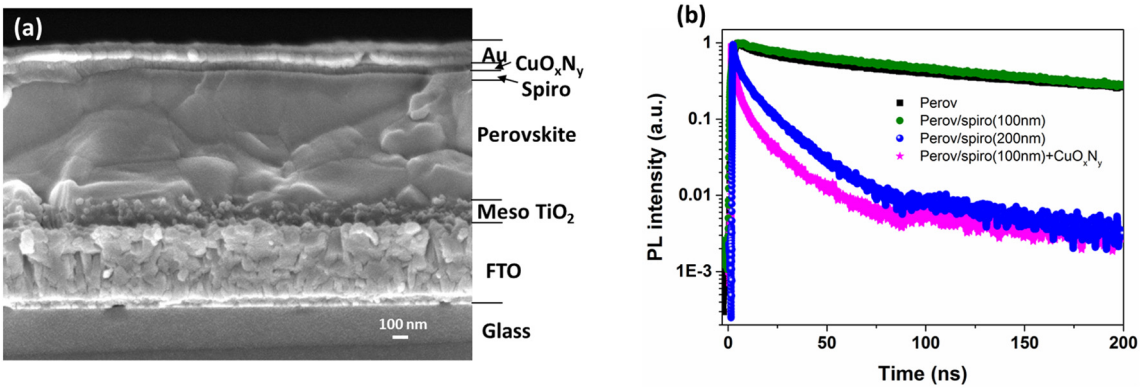


**Fig. 3.** (a) Field emission scanning electron microscopy (FESEM) images of the cross-section of typical perovskite solar cell; (b) Time resolution photoluminescence (TRPL) analysis of perovskite films with different hole transporting layers, lifetime is calculated by fitting the data with bi-exponential equation of $y = y_0 + A_1e^{-(x-x_0)/t1} + A_2e^{-(x-x_0)/t2}$.

shown in Fig. 2(b). The efficiency of all devices exhibits a narrow distribution within the range of 14% to 15%, with an average value of 14.70%. The current-voltage (*I-V*) curve of the champion cell is given in Fig. 2(c), demonstrated a $V_{oc}$ of 1.04 V, $J_{sc}$ of 19.84 mA/cm$^2$, *FF* of 75.87% and efficiency of 15.73%, significantly higher than the reported value of 8.93% [22] with sputtered cuprous oxide. The incident photon-to-current efficiency (IPCE) measurement indicates around 80% quantum efficiency with an integrated current density of 19.45 mA/cm$^2$, which matches well with the *I-V* measurement (Fig. 2(d)).

From a cross section of the microstructure (Fig. 3(a)), the capping layer of perovskite on top of mesoporous $TiO_2$ is around 500 nm. This is followed by a thin ~100 nm layer of Spiro-MeOTAD with no clear interface to the perovskite layer below. The $CuO_xN_y$ layer grows in a columnar microstructure (seen more clearly at increased thickness, as in Fig. S5) with good adhesion to the Spiro-MeOTAD layer, likely facilitating charge transport.

To further investigate the working mechanism, time resolved photoluminescence (TRPL) was performed on perovskite films with and without different HTM layers. A bi-exponential decay equation of $y = y_0 + A_1e^{-(x-x_0)/t1} + A_2e^{-(x-x_0)/t2}$ is employed to fit the measured data (Fig. 3(b)) and the extracted exciton lifetimes are listed in Table S1. Bare perovskite film on glass gives a fluorescence lifetime of 484 ns, which signifies good quality film. When a layer of 100 nm-thick Spiro-MeOTAD is added on top, the fluorescence lifetime decreases to 262 ns, suggesting charge separation at the interface is taking place. Possibly due to the thin Spiro-MeOTAD layer, hole transport is not very efficient. When the Spiro-MeOTAD layer thickness is increased to 200 nm (which is the thickness for normal devices), the lifetime dramatically decreases to 15 ns, indicating efficient quenching due to better charge extraction by this thicker Spiro-MeOTAD layer. Interestingly, when 100 nm-thick Spiro-MeOTAD and sputtered $CuO_xN_y$ are used as the HTM, the fluorescence lifetime is just 11 ns, even lower than that with 200 nm Spiro-MeOTAD. This result provides strong support that $CuO_xN_y$ combined with a thin layer of Spiro-MeOTAD is an efficient hole acceptor for perovskites.

In summary, we have investigated the usage of nitrogen doped cuprous oxide as a hole transporting material for perovskite solar cells. The highest efficiency of 15.73% is achieved with nitrogen doped low power sputtered $CuO_xN_y$ and a thin Spiro-MeOTAD interfacial layer, which is much higher than the reported value of 8.93% with similar process. Time resolved photoluminescence and Hall measurements confirmed the efficient charge transfer between perovskite and $CuO_xN_y$-based HTM, and high conductivity of nitrogen doped cuprous oxide. This work demonstrates the first successful case of using sputtered cuprous oxide as a cheaper and efficient hole transporting material for perovskite solar cell. However, further work on the interface should be performed to eventually eliminate the usage of the interfacial modifier.

## Acknowledgements

The authors acknowledge funding from the National Research Foundation, Prime Minister's Office, Singapore under its Competitive Research Program (CRP Award No. NRF-CRP14-2014-03) and through the Singapore-Berkeley Research Initiative for Sustainable Energy (SinBeRISE) CREATE Program; Nanyang Technological University start-up grants (M4080514 and M4081293); the Ministry of Education Academic Research Fund Tier 1 grants (RG184/14, RG166/16 and RG101/15), and Tier 2 grants (MOE2016-T2-1-100, MOE2014-T2-1-044, MOE2015-T2-2-015 and MOE2016-T2-2-012). The authors would like to acknowledge Mr. K. M. Rameshchandra's help in sputtering $CuO_xN_y$ films during the revision of this paper.

## Appendix A. Supplementary data

Supplementary data to this article can be found online at https://doi.org/10.1016/j.scriptamat.2018.04.049.

## References

[1] G. Han, S. Zhang, P.P. Boix, L.H. Wong, L. Sun, S.-Y. Lien, Prog. Mater. Sci. 87 (2017) 246–291.
[2] T.C. Sum, N. Mathews, Energy Environ. Sci. 7 (8) (2014) 2518–2534.
[3] H.J. Snaith, J. Phys. Chem. Lett. 4 (21) (2013) 3623–3630.
[4] H.S. Jung, N.G. Park, Small 11 (1) (2015) 10–25.
[5] T.M. Brenner, D.A. Egger, L. Kronik, G. Hodes, D. Cahen, Nat. Rev. Mater. 1 (2016) 15007.
[6] N.J. Jeon, J.H. Noh, W.S. Yang, Y.C. Kim, S. Ryu, J. Seo, S.I. Seok, Nature 517 (7535) (2015) 476–480.
[7] M. Saliba, T. Matsui, J.-Y. Seo, K. Domanski, J.-P. Correa-Baena, N. Mohammad K, S.M. Zakeeruddin, W. Tress, A. Abate, A. Hagfeldt, M. Gratzel, Energy Environ. Sci. 9 (6) (2016).
[8] N. Ahn, D.-Y. Son, I.-H. Jang, S.M. Kang, M. Choi, N.-G. Park, J. Am. Chem. Soc. 137 (27) (2015) 8696–8699.
[9] B. Wu, H.T. Nguyen, Z. Ku, G. Han, D. Giovanni, N. Mathews, H.J. Fan, T.C. Sum, Adv. Energy Mater. 6 (2016) 1600551.
[10] I. Zarazua, G. Han, P.P. Boix, S. Mhaisalkar, F. Fabregat-Santiago, I. Mora-Seró, J. Bisquert, G. Garcia-Belmonte, J. Phys. Chem. Lett. 7 (2016) 5105–5113.
[11] G. Han, T.M. Koh, S.S. Lim, T.W. Goh, X. Guo, S.W. Leow, R. Begum, T.C. Sum, N. Mathews, S. Mhaisalkar, ACS Appl. Mater. Interfaces 9 (25) (2017) 21292–21297.
[12] Released by National Renewable Energy Laboratory2018.
[13] Y. Rong, L. Liu, A. Mei, X. Li, H. Han, Adv. Energy Mater. 5 (2015) 1501066.
[14] A.S. Subbiah, A. Halder, S. Ghosh, N. Mahuli, G. Hodes, S.K. Sarkar, J. Phys. Chem. Lett. 5 (10) (2014) 1748–1753.
[15] P. Qin, S. Tanaka, S. Ito, N. Tetreault, K. Manabe, H. Nishino, M.K. Nazeeruddin, M. Gratzel, Nat. Commun. 5 (2014) 3834.
[16] N. Arora, M.I. Dar, A. Hinderhofer, N. Pellet, F. Schreiber, S.M. Zakeeruddin, M. Grätzel, Science 358 (2017) 768–771.
[17] J.A. Christians, R.C. Fung, P.V. Kamat, J. Am. Chem. Soc. 136 (2) (2014) 758–764.
[18] S. Chatterjee, A.J. Pal, J. Phys. Chem. C 120 (3) (2016) 1428–1437.
[19] H. Rao, S. Ye, W. Sun, W. Yan, Y. Li, H. Peng, Z. Liu, Z. Bian, Y. Li, C. Huang, Nano Energy 27 (2016) 51–57.
[20] W. Sun, Y. Li, S. Ye, H. Rao, W. Yan, H. Peng, Y. Li, Z. Liu, S. Wang, Z. Chen, L. Xiao, Z. Bian, C. Huang, Nanoscale 8 (20) (2016) 10806–10813.

[21] W. Yu, F. Li, H. Wang, E. Alarousu, Y. Chen, B. Lin, L. Wang, M.N. Hedhili, Y. Li, K. Wu, X. Wang, O.F. Mohammed, T. Wu, Nanoscale 8 (11) (2016) 6173–6179.
[22] W. Du, J. Yang, C. Xiong, Y. Zhao, X. Zhu, Int. J. Mod. Phys. B 31 (16–19) (2017) 1744065.
[23] Y. Zhou, Z. Zhou, M. Chen, Y. Zong, J. Huang, S. Pang, N.P. Padture, J. Mater. Chem. A 4 (45) (2016) 17623–17635.
[24] J. T-Thienprasert, S. Limpijumnong, Appl. Phys. Lett. 107 (22) (2015) 221905.
[25] Z. Zhao, X. He, J. Yi, C. Ma, Y. Cao, J. Qiu, RSC Adv. 3 (1) (2013) 84–90.
[26] Y. Wang, J. Ghanbaja, D. Horwat, L. Yu, J.F. Pierson, Appl. Phys. Lett. 110 (13) (2017), 131902.